THE JOURNAL OF BIOLOGICAL CHEMISTRY
Vol. 278, No. 40, Issue of October 3, pp. 38292–38300, 2003

Printed in U.S.A.

An Intron Is Required for Dihydrofolate Reductase Protein Stability*

Received for publication, December 13, 2002, and in revised form, June 20, 2003
Published, JBC Papers in Press, July 15, 2003, DOI 10.1074/jbc.M212746200

Véronique Noé‡§, Simon MacKenzie¶, and Carlos J. Ciudad‡

From the ‡Department of Biochemistry and Molecular Biology, School of Pharmacy, University of Barcelona E-08028 and the ¶Department of Cellular Biology, Physiology and Immunology, School of Sciences, Autonomous University of Barcelona, E-08193 Barcelona, Spain

We compared the expression of *dihydrofolate reductase* minigenes with and without an intron. The levels of protein were significantly higher in the presence of *dihydrofolate reductase* intron 1. However, mRNA levels in both constructs were comparable. In addition, the RNA transcribed from either construct was correctly polyadenylated and exported to the cytoplasm. The intron-mediated increase in dihydrofolate reductase protein levels was position-independent and was also observed when *dihydrofolate reductase* intron 1 was replaced by heterologous introns. The translational rate of dihydrofolate reductase protein was increased in transfectants from the intron-containing minigene. In addition, the protein encoded by the intronless construct was unstable and subject to lysosomal degradation, thus showing a shorter half-life than the protein encoded by the intron-containing minigene. We conclude that an intron is required for the translation and stability of dihydrofolate reductase protein.

Minigenes derived from intron-containing genes are usually expressed more efficiently than their intronless counterparts (1, 2, 3). This enhanced expression could be because of the presence of intronic enhancers of transcription, the facilitation of polyadenylation by an upstream intron (4–9), or a requirement for intron removal for the export of mRNA from the nucleus or its stability in the nucleus (10–13). The transcriptional history of pre-mRNA can also influence the subsequent translation of the mRNA in the cytoplasm (14, 15). Another example of a cytoplasmic process that depends on the initial presence of an intron is the nonsense-mediated decay of mRNA (16, 17).

Efficient transfection by minigenes for dihydrofolate reductase (DHFR)[1] depends on the presence of an intron (18–20). This requirement can be met by the inclusion of a single intron in mouse or hamster *dhfr* minigenes. The 300-bp intron 1 suffices and is the intron usually included in *dhfr* minigenes. This is also the intron that is removed last (21). We have used this intron-dependent expression of DHFR as a model system to determine the mechanisms linking intron removal to other aspects of gene expression. Surprisingly, we found that intron removal can influence a cytoplasmic event that is further downstream than translation: the degradation of newly synthesized protein.

MATERIALS AND METHODS

Plasmid Constructions

The starting construct, pDCH1P11, containing the six exons of the hamster *dhfr* gene, intron 1, about 400 bp of the 5′-flank, and the first of the three polyadenylation sites in exon 6, was constructed by cloning the *Sma*I-*Hin*dIII fragment from hamster minigene pDCH2 (19) into the *Sma*I-*Hin*dIII sites of the cloning vector pSP72 (Promega). The construct pDCHIP10 corresponding to the intronless version of pDCH1P11 was constructed by cloning the *Sma*I-H*in*dIII fragment from hamster minigene pDCH0 (19) into the *Sma*I-*Hin*dIII sites of pSP72. All other minigenes were derived from pDCH1P11 and pDCH1P10, as described below and illustrated in Fig. 1.

pDSV11 was constructed by digesting pDCH1P11 with *Bam*HI and *Hin*dIII to remove the 3′-UTR sequence containing *dhfr* polyadenylation site 1. The linearized plasmid was then ligated with a *Bam*HI-*Hin*dIII fragment of 461 bp from vector pUDH10-3 (22) containing the SV40 late polyadenylation sequence. pDSV10 was constructed from pDCH1P10 using the same strategy described above for pDSV11.

pDAPRT—Hamster *adenine phosphoribosyltransferase (aprt)* intron 3 was PCR-amplified from the *aprt* gene template plasmid, pWTaprt (23), using primers modified to contain an *Msc*I site just upstream and an *Eco*RI site just downstream of the intron sequence. After digestion of the PCR fragment with *Msc*I and *Eco*RI, the 155-bp product was cloned into the *Msc*I-*Eco*RI sites bordering intron 1 in pDCH1P11.

pDGlobin was constructed using the same strategy described above for pDAPRT. Human *β-globin* intron 3 was PCR-amplified from a globin plasmid using modified primers to produce an *Msc*I site and an *Eco*RI site flanking the intron sequence. After digestion of the PCR fragment with *Msc*I and *Eco*RI, the 130-bp product was cloned in the *Msc*I-*Eco*RI sites of pDCH1P11.

pDCH1P10–5′UTR—A 322-bp fragment from *dhfr* minigene pDCH1P11 was PCR-amplified using primers of a modified sequence to produce an *Avr*II site just upstream and downstream of *dhfr* intron 1 sequence. After digestion of the PCR fragment with *Avr*II, the 312-bp product was cloned in the *Avr*II site in the *dhfr* 5′-UTR in pDCH1P10.

Cell Culture and Transfection

Monolayer cultures of CHO DG44 cells (24) were grown in Ham's F12 medium (Invitrogen) supplemented with 7% fetal bovine serum (fetal bovine serum; Invitrogen) and maintained at 37 °C in a humidified 5% CO_2-containing atmosphere.

Transfections of the *dhfr* minigenes were carried out by the calcium phosphate method (25). A mixture consisting of 2 μg of the *dhfr* construct, 0.4 μg of pBPV-neo (26), and 17.6 μg of carrier calf thymus DNA (Invitrogen) per 10-cm-diameter tissue culture dish was used. After 5 h of exposure to DNA and 24 h of expression in non-selective medium, transfectants that had received the *neo* gene were selected in 400 μg of active G418 (Invitrogen) per ml. Colonies were pooled, expanded, and then used for preparation of RNA and cytoplasmic extracts.

* This work was supported by Grant SAF2002–00363 from Comisión Interministerial de Ciencia y Tecnología and Grant 2001SGR141 from Comissió Interdepartamental de Recerca i Innovació Tecnològica. The costs of publication of this article were defrayed in part by the payment of page charges. This article must therefore be hereby marked "*advertisement*" in accordance with 18 U.S.C. Section 1734 solely to indicate this fact.

§ To whom correspondence should be addressed: Dept. of Biochemistry and Molecular Biology, School of Pharmacy, University of Barcelona, Av. Diagonal 643, Barcelona E-08028, Spain. Tel.: 34-93-403-4455; Fax: 34-93-402-1896; E-mail: noe@farmacia.far.ub.es.

[1] The abbreviations used are: DHFR, dihydrofolate reductase; UTR, untranslated region; aprt, adenine phosphoribosyltransferase; CHO, Chinese hamster ovary.

DHFR Activity Assay

Transfection experiments were carried out in *dhfr*-deficient cells (CHO-DG44) using the FuGENE 6 transfection reagent (Roche Applied Science). DG44 cells (225,000) were plated in 35-mm dishes; after 18–20 h they were transfected with 2 μg of *dhfr* minigenes, pDCHIP11 or pDCHIP10, mixed with 3 μl of FuGENE 6. After 24 h the medium was replaced with selective −GHT medium, lacking glycine, hypoxanthine, and thymidine, the final products of DHFR activity. The resulting DHFR activity was determined by the net incorporation of radioactive deoxyuridine (6-[^{3}H]deoxyuridine; NEN Dupont) into cellular DNA as described in Ref. 27.

Cell Fractionation

Cell pellets (2×10^7) were resuspended in 5 ml of hypotonic buffer (HB, 15 mM NaCl, 15 mM Tris-HCl, 0.5 mM EDTA, 60 mM KCl, 100 mM phenylmethylsulfonyl fluoride, 1 mM β-mercaptoethanol, pH 8) and incubated at 4 °C for 5 min. Cells were pelleted for 5 min at $800 \times g$ and lysed by the addition of 100 μl of HB buffer supplemented with 0.1% Triton X-100 (Sigma). Nuclei were pelleted for 10 min at $1000 \times g$ and separated from the supernatant corresponding to the cytoplasmic fraction. Nuclei were washed once in HB buffer without detergent and pelleted as before to obtain the nuclear fraction.

Protein Analysis

Cytoplasmic extracts (100 μg) from cells permanently transfected with the different *dhfr* minigenes were subjected to electrophoresis in an SDS-12% polyacrylamide gel (28) and transferred to a polyvinylidene difluoride membrane (Immobilon P; Millipore) using a semidry electroblotter. The membrane was probed with a polyclonal rabbit antibody raised against purified recombinant Chinese hamster DHFR (1:500 dilution). Signals were detected by secondary horseradish peroxidase-conjugated antibody (1:5000 dilution) and enhanced chemiluminescence as recommended by the manufacturer (Amersham Biosciences). The antibody detected a band of the expected molecular mass (21,000 kDa) in extracts of DHFR-positive cells, and no band was detected in cells carrying a double deletion of the *dhfr* gene (data not shown).

The stability of DHFR protein was assessed by calculating its half-life from the amount of remnant protein at various times after addition of cycloheximide to the cell culture. Cytoplasmic extracts from cells permanently transfected with pDCH1P11 or pDCH1P10 were prepared and analyzed by Western blot. The blot corresponding to pDCH1p10 was probed with the antibody against Chinese hamster DHFR at 1:250 dilution and with the secondary peroxidase-conjugated antibody at 1:2000 dilution to increase the resulting DHFR signal.

The following inhibitors of proteolysis were added to the cell cultures to determine their effect on DHFR protein levels, leupeptin, E64, MG132 (all from Calbiochem) and a protease mixture inhibitor (Sigma). The inhibitors were dissolved in Me_2SO and stored at −20 °C.

Cell Labeling and Immunoprecipitation

Transfectants from pDCHIP11 and pDCHIP10 (5×10^5 cells) were plated in 35-mm dishes, and after 18 h the medium was replaced with methionine- and cysteine-free Dulbecco's modified Eagle's medium (Invitrogen) supplemented with 7% dialyzed fetal bovine serum. The cells were starved in this medium for 90 min, and at the end of this time they were pulse-labeled for 90 min with 150 μCi/ml [^{35}S]cysteine/methionine (Promix L-[^{35}S] *in vitro* cell-labeling mix from Amersham Biosciences). After the pulse, the medium was removed, the cells were washed twice with Ham's F-12 medium, and then chased for different periods of time in F-12 medium supplemented with 2 mM methionine and 2 mM cysteine. After the chase, the cells were harvested by trypsinization and washed in 1 ml of hypotonic buffer (HB, 15 mM NaCl, 15 mM Tris-HCl, 0.5 mM EDTA, 60 mM KCl, 100 mM phenylmethylsulfonyl fluoride, 1 mM β-mercaptoethanol, pH 8). Cells were pelleted for 5 min at $800 \times g$ and lysed by the addition of 100 μl of HB buffer supplemented with 0.1% Nonidet P-40 (Sigma), 20 μg/ml leupeptin, 2 μg/ml aprotinin, and 20 nM benzamidine. Nuclei were pelleted for 10 min at $1000 \times g$ and separated from the radiolabeled supernatant corresponding to the cytoplasmic fraction. DHFR protein was immunoprecipitated from the cytoplasmic fraction by the addition of a specific antibody against hamster DHFR for 3 h at 4 °C. The resulting immunocomplex was recovered by the addition of 30 μl of a 50% (v/v) suspension of protein A-agarose (Roche Applied Science), followed by an additional incubation for 3 h at 4 °C. After centrifugation, the pellets were washed twice with phosphate-buffered saline supplemented with 0.3 M NaCl and 0.1% Nonidet P-40. DHFR protein was eluted by boiling for 5 min in protein loading buffer and analyzed in an SDS-15% polyacrylamide gel. After electrophoresis, the gel was dried and the radiolabeled protein was quantitated by phosphorimaging.

To determine the translational rate of DHFR protein in transfectants from pDCH1P11 and pDCH1P10, the cells were labeled for different periods of time with 150 μCi/ml [^{35}S]cysteine/methionine. After the labeling, the cells were harvested by trypsinization, and cytoplasmic extracts were prepared as described above. DHFR protein was immunoprecipitated, and after electrophoresis the radiolabeled protein was quantitated by phosphorimaging.

RNA Analysis

Total, cytoplasmic, and nuclear RNA were extracted from the transfectant populations using the Ultraspec™ RNA reagent (Biotecx) in accordance with the manufacturer's instructions. cDNA was synthesized in a 20-μl reaction mixture containing 1 μg of RNA, 125 ng of random hexamers (Roche Applied Science), 10 mM dithiothreitol, 20 units of RNasin (Promega), 0.5 mM dNTPs (Applichem), 4 μl of 5× RT buffer, 200 units of M-MLV reverse transcriptase (above two from Invitrogen). The reaction mixture was incubated at 37 °C for 60 min. Five μl of the cDNA mixture was used directly for PCR amplification.

PCR reactions were typically carried out as follows. A standard 50-μl mixture contained 5 μl of the cDNA mixture, 4 μl of 10× PCR buffer (Mg^{2+}-free), 1.5 mM $MgCl_2$, 0.2 mM dNTPs, 2.5 μCi of α-[^{32}P]dATP (3000 Ci/mmol, Amersham Biosciences), 2.5 units of *Taq* polymerase (Ecogen), and 500 ng of each of four primers. The primers used were: 5′-AAGAACGGAGACCTTCCCTG-3′ in exon 1 and 5′-GAACTGCCTCCAACTATC-3′ in exon 4 for DHFR mRNA and 5′-ATCCGCAGTTTCCCCCGACTT-3′ in exon 1 and 5′-TCACACACTCCACCACCTCA-3′ in exon 5 for APRT mRNA as an internal control.

The reaction mixture was separated in two phases by a solid paraffin wax layer (melting $T = 58–60$ °C; Fluka) that prevents complete mixing of PCR reactants until the reaction has reached the temperature at which nonspecific annealing of primers to non-target DNA is minimal. The lower solution contained the $MgCl_2$, the dNTPs, the four primers, the α-[^{32}P]dATP. and half of the buffer, and the upper solution contained the cDNA, the *Taq* enzyme, and the remaining buffer. PCR was performed for 23 cycles, after 1 min of denaturation at 94 °C; each cycle consisted of denaturation at 92 °C for 1 min, primer annealing at 59 °C for 75 s, and primer extension at 72 °C for 110 s. Five μl of each PCR sample was electrophoresed in a 5% polyacrylamide gel. The gel was dried, and the radioactive bands were visualized by autoradiography.

RNase Protection Analysis

Uniformly ^{32}P-labeled antisense RNA probes for the mapping of DHFR transcripts were synthesized from pDCH1P11 and pDSV11 linearized with *Bam*HI using Sp6 RNA polymerase and the RiboScribe™ Sp6 RNA probe synthesis kit (Epicenter Technologies) in accordance with the manufacturer's instructions. *In vitro* transcription was performed in 20 μl using 1 μg of linearized plasmid DNA, 50 μCi of α-[^{32}P]GTP (NEN Dupont), 10 μM GTP, 500 μM each of ATP, CTP, and UTP, and 40 units of Sp6 RNA polymerase.

RNase protection assays were performed with 10 or 20 μg of total RNA using the RPAIII kit (Ambion) as specified by the manufacturer. Briefly, total RNA was hybridized to DHFR pA1 or SV40 pA *in vitro* synthesized antisense RNAs (8×10^4 cpm) in 20 μl overnight at 42 °C and subsequently treated with RNase A (25 units/ml) and RNase T1 (100 units/ml) for 1 h at 37 °C. Protected fragments were precipitated, electrophoresed in 5% denaturing polyacrylamide gels, and visualized by phosphorimaging after the gel was dried.

Polyadenylation Analysis

Poly(A) length analysis of the different mRNA species was performed by RT-PCR following the method of Sallés *et al.* (29) with modifications described in Ref. 30. Briefly, 2 μg of total RNA from each transfectant was used in the RT reaction with 1 μg of primer consisting of a specific arbitrary sequence followed by oligo(dT)$_{12}$. The RNA and the primer were heated to 80 °C for 5 min, cooled to room temperature (0.5 °C/min), and then placed at 4 °C. The remaining components of the RT reaction were then added. The RT reaction was performed for 5 min at 4 °C, 5 min at room temperature, 5 min at 37 °C, and 45 min at 42 °C. Five μl of the RT reaction was then used in the PCR, which was performed with a 5′-primer upstream of either the *dhfr* polyadenylation site 1 or the SV40 polyadenylation site and an oligomer corresponding to the arbitrary sequence of the RT primer as the 3′-primer. PCR was carried out as described above for 30 cycles. The PCR products were electrophoresed and visualized by autoradiography. The length of the poly(A) tails

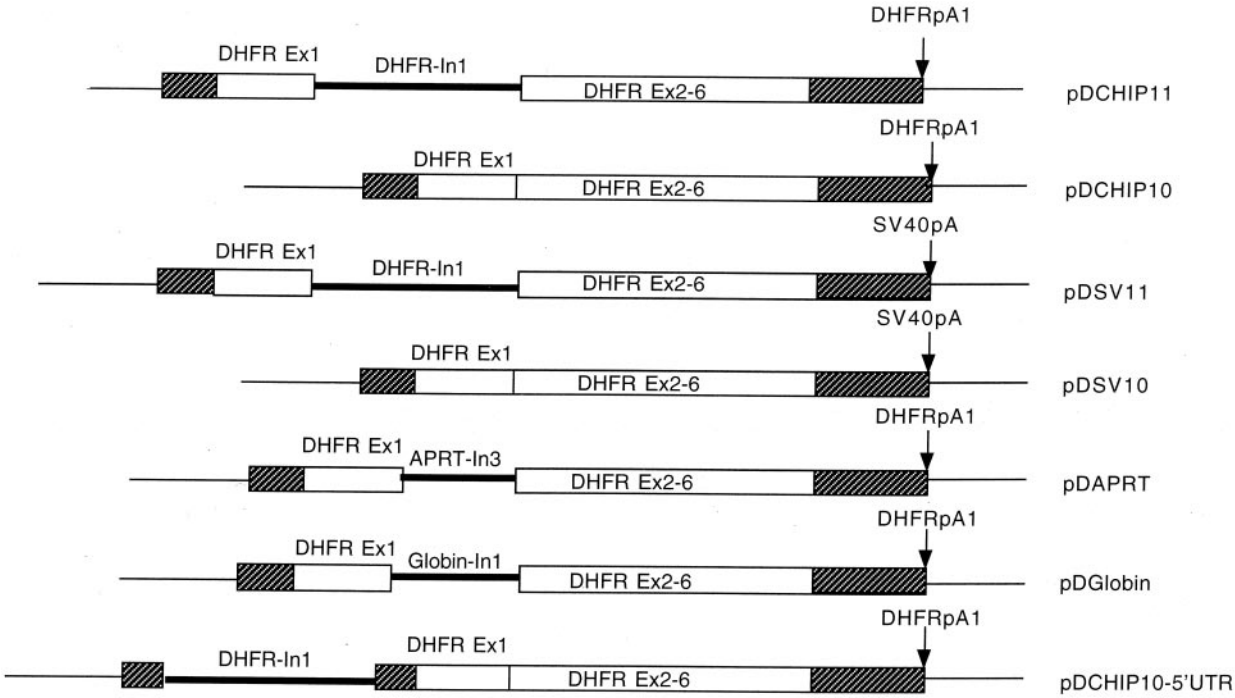

FIG. 1. ***Dhfr* minigenes.** *White boxes* represent exons, with *shaded areas* indicating the 5′-untranslated region. *Thick black lines* represent introns. The *arrows* indicate polyadenylation sites (*pA*). The distinctive features of each construct are as follows: pDCH1P11 contains intron 1 and the first polyadenylation site of the hamster *dhfr* gene. pDCH1P10 lacks intron 1. pDSV11 and pDSV10 contain the same minigenes as pDCH1P11 and pDCH1P10, respectively, but the first polyadenylation site of the hamster *dhfr* gene has been replaced by the SV40 late polyadenylation sequence in these constructs. pDAPRT contains hamster *aprt* intron 3 and pDGlobin contains human *β-globin* intron 3 instead of *dhfr* intron 1 as intronic sequences. 5′-UTR-I1-pDCH1P10 contains *dhfr* intron 1 in the 5′-UTR of the minigene pDCH1P10.

was determined from the length of the smear of the PCR products.

The primer used in the RT reaction was 5′-GCGAGCTCCGCGGCCGCG$(T)_{12}$-3′, and the primers used in the PCR reaction were 5′-TAGAGAGGGATAGTTAGGAAGATG-3′ upstream of the polyadenylation sites and 5′-GCGAGCTCCGCGGCCGCG-3′ as the reverse primer.

RESULTS

Efficient Expression of DHFR Protein from a Minigene Requires an Intron—To study the relationship between intron removal and *dhfr* gene expression, we used several *dhfr* minigenes that either lacked all 5 *dhfr* introns or contained a single intron. All minigenes were driven by the *dhfr* promoter and contained either the first *dhfr* polyadenylation site or the SV40 late polyadenylation site. The minigenes that were used in these analyses are summarized in Fig. 1.

DHFR-deficient cells do not grow in a medium lacking the end products of one-carbon metabolism glycine, purines, and thymidine (−GHT medium). The ability of a transfected *dhfr* minigene to confer a DHFR-positive growth phenotype (ability to grow in −GHT medium) to DHFR-deficient CHO cells depends on the presence of one or more introns (18, 19, 31). Whereas an intron-containing plasmid produced the expected frequency of colonies ($\sim 10^{-4}$ colony/recipient cell), an intronless counterpart yielded 3 to 6% of this number.

For a more direct estimate of DHFR enzyme activity, we measured the incorporation of radioactive deoxyuridine into cellular DNA, a process that requires DHFR. DG44 cells were transfected with pDCHIP11 or pDCHIP10 (Fig. 1), and after 24 h of expression the incorporation of radioactive deoxyuridine was measured. The intron-containing pDCHIP11 produced measurable DHFR activity, whereas the incorporation in the case of the intronless pDCHIP10 was at the level of background (Fig. 2*A*).

The low level of DHFR activity in cells transfected with the intronless minigene could be due either to a lower level of DHFR protein in these cells or to a defective enzyme. To distinguish between these two possibilities we determined the levels of DHFR protein in cytoplasmic extracts from transfectants by Western blotting using an anti-hamster DHFR antibody. For these experiments, in addition to pDCHIP11 and pDCHIP10, we used plasmids in which the SV40 late polyadenylation site was substituted for the *dhfr* polyadenylation site. The *dhfr* polyadenylation site 1 is relatively weak; the stronger SV40 polyadenylation site affords a higher level of gene expression (Ref. 30 and see below). Cells transfected with the intronless versions of the minigenes produced barely detectable levels of DHFR, compared with the strong signals yielded by the intron-containing minigenes (Fig. 2*B*). This result indicates that the lack of DHFR activity was because of the absence of DHFR protein in these transfectants. Replacement of the *dhfr* polyadenylation site by the SV40 site in the minigenes increased the levels of protein, although the effect on the intron-containing gene was stronger.

DHFR mRNA Levels Do Not Depend on the Presence of an Intron—We next analyzed the levels of DHFR mRNA in pooled permanent transfectants to determine whether the absence of protein in transfectants from the intronless minigenes was because of a decreased level of DHFR mRNA in these cells. Total RNA was extracted from cells transfected with pDCH1P11, pDCH1P10, pDSV11, or pDSV10, and DHFR mRNA was detected by quantitative RT-PCR. Surprisingly enough, DHFR mRNA levels yielded by the intronless minigene pDCH1P10 were comparable with those given by the intron-containing minigene pDCH1P11 (Fig. 3*A*). The replacement of *dhfr* pA1 by the late polyadenylation sequence from SV40 increased the total levels of DHFR mRNA 2-fold for the intron-containing pDSV11 minigene, and to a lesser extent for the intronless minigene. Although there was some decrease in the level of total DHFR mRNA in the case of the intronless pDSV10 minigene compared with the pDSV11 construct (Fig.

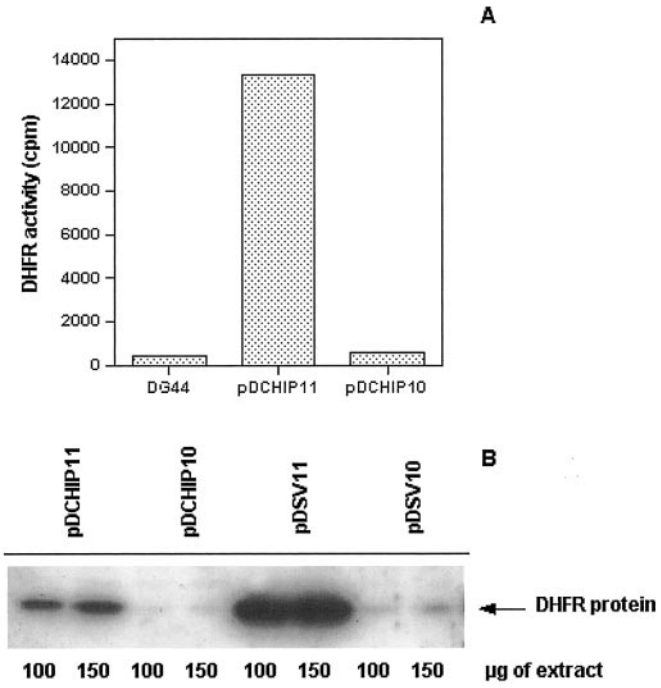

FIG. 2. **DHFR activity and protein levels in permanent transfectants.** *A*, DHFR activity in transient transfections with pDCHIP11 and pDCHIP10. DG44 cells were transfected with 2 μg of *dhfr* minigene plasmids mixed with 3 μl of FuGENE 6 per 35-mm dish. After 24 h of expression, the resulting DHFR activity was determined by the incorporation of radioactive deoxyuridine into cellular DNA as described under "Materials and Methods." *B*, DHFR protein levels in pooled permanent transfectants. Cytoplasmic extracts (100–150 μg) from the indicated transfectants were resolved by SDS-acrylamide gel electrophoresis and subjected to Western blot analysis using an antibody against hamster DHFR.

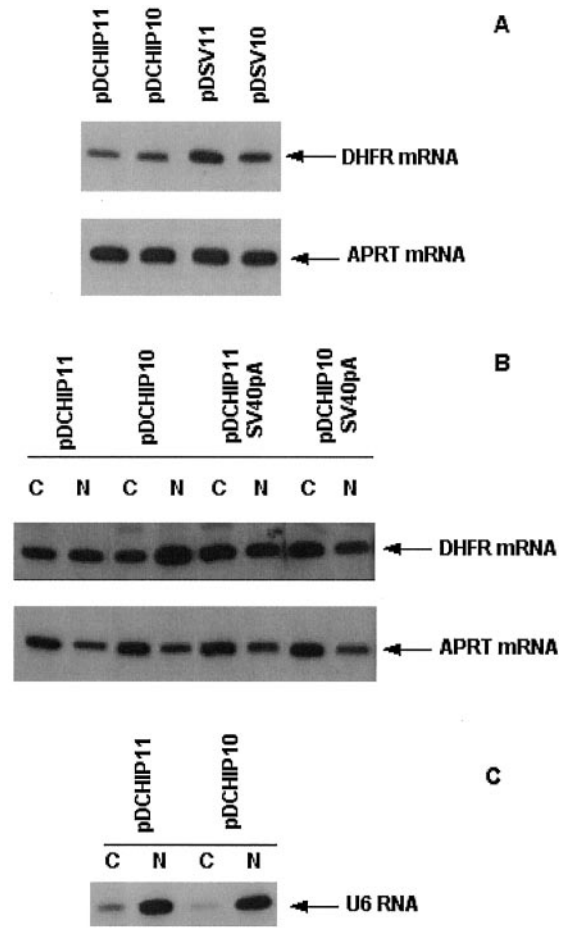

FIG. 3. **DHFR mRNA levels in permanent transfectants.** *A*, DHFR mRNA levels. Total RNA was extracted from the indicated pooled permanent transfectants, and the levels of DHFR mRNA were determined by quantitative RT-PCR as described under "Materials and Methods." As an internal control of both the RT and the PCR reactions, APRT mRNA also was amplified. A representative autoradiogram of the DHFR and APRT RT-PCR products is shown. *B*, cellular distribution of DHFR mRNA in pooled permanent transfectants. Cytoplasmic and nuclear RNA were extracted from the different transfectants, and the levels of DHFR mRNA in these fractions were determined by quantitative RT-PCR, using APRT mRNA as an internal control. Equal amounts of RNA were used in the determination. A representative autoradiogram of the DHFR and APRT RT-PCR products is shown. *C*, cellular distribution of U6 mRNA. As a control for nuclear integrity, the levels of U6 mRNA were measured by quantitative RT-PCR in RNA samples from cytoplasmic and nuclear fractions from pooled permanent transfectants of pDCH1P11 and pDCH1P10.

3*A*), the effect was small compared with the difference in DHFR protein level (compare Fig. 2*B*)

Export of DHFR mRNA Does Not Require Splicing in the Nucleus—Many mRNAs transcribed from cDNA derived from intron-containing genes fail to be exported to the cytoplasm in the absence of splicing (4, 10–13). The resulting lack of cytoplasmic mRNA could explain the low level of DHFR protein in transfectants of the intronless minigene. We therefore analyzed the cellular distribution of DHFR mRNA encoded by either the intron-containing or the intronless minigenes. As can be seen in Fig. 3*B*, the level of nuclear DHFR mRNA was increased 3-fold in cells transfected with pDCH1P10 compared with the other transfectants; the replacement of the *dhfr* polyadenylation site by the SV40 site in pDSV10 abolished this effect. It may be that in the absence of a strong polyadenylation site, the presence of an intron can facilitate the nuclear export of DHFR mRNA, as was found in the several cases cited above. However, DHFR mRNA levels in the cytoplasm were similar in all transfectants either in the presence or in the absence of an intron in the corresponding minigene. These results suggested that the low levels of DHFR protein produced by the intronless minigenes were not because of defective export of DHFR mRNA.

To rule out the possibility that the cytoplasmic DHFR mRNA signal from the intronless minigenes was because of a nuclear contamination, we examined the distribution of U6 small nuclear RNA in the different subcellular fractions to test for nuclear integrity (32). U6 snRNA participates in pre-mRNA splicing and is not known to have a cytoplasmic phase (33). Almost all of the U6 snRNA was confined to the nuclear fraction (Fig. 3*C*), indicating that the signal for DHFR mRNA in the cytoplasm of transfectants of the intronless minigene was not because of nuclear leakage.

DHFR mRNA Is Correctly Polyadenylated in the Absence of an Intron—We next considered the possibility that the absence of an intron leads to poor or no polyadenylation (9), which could lead to deficiencies in translation initiation (34–36). Polyadenylation of DHFR mRNA transcripts was analyzed by two methods. First, to determine whether the transcripts were correctly cleaved, the 3′-ends of DHFR transcripts that derived from the different *dhfr* constructs were mapped by RNase protection using probes that spanned either the *dhfr* or the SV40 polyadenylation sites. As can be seen in Fig. 4*A*, RNA from pDCH1P11 and pDCH1P10 transfectants both protected a fragment of the *dhfr* probe that migrated at 138 nt, as expected from the position of *dhfr* polyadenylation site 1 (19). RNA from pDSV11 and pDSV10 transfectants both protected a fragment of the SV40 pA probe that migrated at 136 nt, the size expected for polyadenylation at the late SV40 polyadenylation site. Thus, both the intron-containing and the intronless transcripts were cleaved at the expected sites during 3′-end proc-

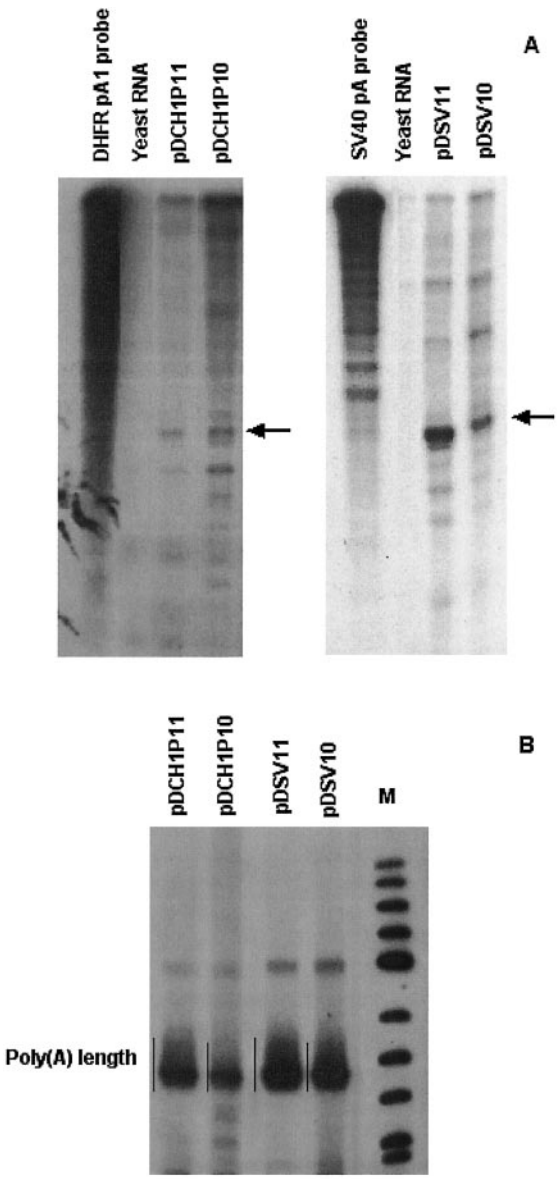

FIG. 4. **Polyadenylation of DHFR mRNA.** *A*, total RNA was isolated from pooled permanent transfectants of pDCH1P11, pDCH1P10, pDSV11, and pDSV10 constructs. DHFR transcripts were mapped by hybridization to antisense RNA probes. The probe for the DHFR polyadenylation site consisted of a uniformly ^{32}P-labeled antisense transcript of 576 nt, 560 nt derived from *dhfr* gene sequences, of which 138 nt correspond to the 3′-UTR and 422 nt to 3′-flanking DNA. The probe for the late SV40 polyadenylation site consisted of a uniformly ^{32}P-labeled antisense transcript of 477 nt, 461 nt derived from SV40 sequences, of which 136 nt correspond to the 3′-UTR and 325 nt to 3′-flanking DNA. Before electrophoresis, samples were treated with a mixture of RNases A and T1. As a control for probe integrity, 1/10 of each of the input RNA probes was electrophoresed without exposure to RNase. Fragments of each probe that were protected by DHFR transcripts are indicated by *arrows*. Transcripts from pDCH1P11 and pDCH1P10 protected a fragment of 138 nt; transcripts from pDSV11 and pDSV10 protected a fragment of 136 nt. The additional bands that can be seen are not specifically protected by DHFR mRNA, because they also appeared using yeast RNA as a control. *B*, 2 μg of total RNA from the indicated transfectants were subjected to RT-PCR, as described under "Materials and Methods." The RT primer was comprised of an oligo(dT) sequence preceded by a particular arbitrary sequence. The oligo(dT) can prime from a variety of positions within the poly(A) tail, giving rise to a mixture of products of different lengths. The PCR was performed with a 5′-primer upstream of the first *dhfr* polyadenylation site or the SV40 polyadenylation site and a 3′-primer corresponding to the arbitrary sequence in the RT primer. The amplified products were visualized by autoradiography after gel electrophoresis. The length of the poly(A) tails was determined from the length of the smears, indicated with *vertical lines* between the lanes.

essing. Second, to determine the poly(A) length in DHFR mRNA, a method based on RT-PCR was used (30). The RT reaction was performed with a primer containing an oligo(dT) sequence that can initiate polymerization along the length of the poly(A) tail. The PCR was carried out with a 5′-primer specific for DHFR and with a 3′-primer corresponding to an arbitrary sequence included at the start of the RT primer. Under these conditions, the length of the smear of the amplified products indicates the length of the poly(A) tail in each case. We analyzed the poly(A) length for polyadenylation sites in RNA samples from the different transfectants. For construct pDCH1P11, the poly(A) tail at *dhfr* polyadenylation site 1 was 65 nt, in accordance with previous results (30). Using the pDCH1P10 construct we found that the poly(A) tail was 53 nt. In the case of constructs pDSV11 and pDSV10, the poly(A) tails at the late SV40 polyadenylation site were 78 and 65 nt, respectively (Fig. 4*C*). We concluded that poly(A) tails are added to DHFR mRNA molecules derived from both intron-containing and intronless transcripts, but that the length of the poly(A) tail may be somewhat longer when an intron was initially present.

Intron Requirements for the Accumulation of DHFR—The requirement of *dhfr* intron 1 for DHFR protein accumulation could depend on the presence of a specific RNA sequence in this intron or on the passage of the transcript through the splicing process. We distinguished between these two possibilities by replacing *dhfr* intron 1 with heterologous introns of comparable size. We constructed two new *dhfr* minigenes, pDAPRT and pDGlobin, in which *dhfr* intron 1 was replaced by hamster adenine phosphoribosyltransferase intron 3 or human β-globin intron 1, respectively. These minigenes were transfected into DG44 cells, and pooled permanent transfectants were analyzed for their DHFR mRNA and protein levels. As can be seen in Fig. 5*A*, the substitution of *dhfr* intron 1 by heterologous introns yielded increased levels of total DHFR mRNA compared with pDCH1P11 (Fig. 5*A*) and comparable amounts of DHFR mRNA in the cytoplasm (Fig. 5*B*). The heterologous introns were not spliced as efficiently as the endogenous intron; unspliced DHFR pre-mRNA accumulated in the nucleus in transfectants of pDAPRT and pDGlobin (Fig. 5*B*). This restriction of unspliced RNA to the nucleus was an additional indication that little nuclear RNA is leaking into the cytoplasmic fraction in these experiments. From a comparable amount of cytoplasmic mRNA, pDAPRT and pDGlobin minigenes gave rise to even higher amounts of DHFR protein than the pDCH1P11 minigene (Fig. 5*C*). This result suggests that it is the splicing process rather than a specific intronic sequence that underlies increased DHFR protein expression.

We also investigated whether the effect of *dhfr* intron 1 was dependent on the position of the intron in the transcript and, more specifically, whether it could act from a location upstream of the translational start site. For that purpose pDCH1P10-5′-UTR, in which *dhfr* intron 1 was placed in the 5′-UTR of pDCH1P10, was constructed and transfected into DG44 cells. As shown in Fig. 5*D*, pDCH1P10–5′-UTR transcripts in pooled permanent transfectants were correctly spliced and produced a slightly higher amount of DHFR mRNA than the pDCHIP11 construct. The levels of DHFR protein in cytoplasmic extracts from these cells were determined by Western blot, and in accordance with the mRNA levels, DHFR protein levels were also increased in transfectants of pDCH1P10-5′-UTR (Fig. 5*E*).

The Translational Rate of DHFR mRNA Is Decreased in Transfectants Carrying the Intronless Minigene—The simplest explanation for why intronless transcripts yield much lower steady state levels of DHFR protein is that these mRNA mol-

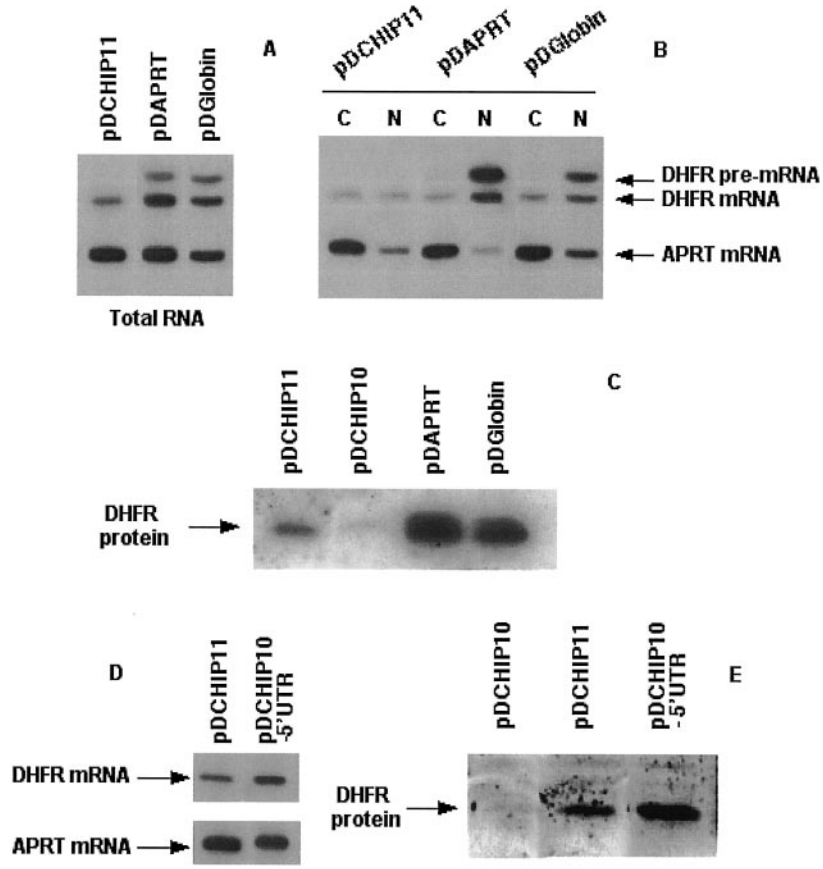

FIG. 5. **DHFR mRNA and protein levels in permanent transfectants from *dhfr* minigenes.** *A*, DHFR mRNA levels. Total RNA from pDCH1P11, pDAPRT, and pDGlobin was extracted and subjected to quantitative RT-PCR to determine DHFR mRNA levels. The signal for APRT mRNA was used as an internal control for the RT-PCR reaction. A representative autoradiogram of the DHFR and APRT RT-PCR products is shown. *B*, cellular distribution of DHFR mRNA in permanent transfectants from pDCH1P11, pDAPRT, and pDGlobin. Cytoplasmic and nuclear RNA from transfectants were subjected to RT-PCR as described under "Materials and Methods." A representative autoradiogram of the amplified products corresponding to DHFR mRNA and APRT mRNA is shown. *C*, DHFR protein levels in permanent transfectants from pDCH1P11, pDCH1P10, pDAPRT, and pDGlobin. Cytoplasmic extracts (100 μg) were resolved by SDS-acrylamide gel electrophoresis and subjected to Western blot analysis using an antibody against hamster DHFR and enhanced chemiluminescence. *D*, DHFR mRNA levels. Total RNA from pDCH1P11 and 5′-UTR/I1/pDCH1P10 was extracted and subjected to quantitative RT-PCR to determine DHFR mRNA levels in these cells. As an internal control of both the RT and the PCR reactions, APRT mRNA also was amplified. A representative autoradiogram of the DHFR and APRT RT-PCR products is shown. *E*, DHFR protein levels in permanent transfectants from pDCH1P11, pDCH1P10, and 5′-UTR/I1/pDCH1P10. 100 μg of cytoplasmic extracts from pDCH1P11, pDCH1P10, and 5′-UTR/I1/pDCH1P10 transfectants were resolved by gel electrophoresis and subjected to Western blot analysis using an antibody against hamster DHFR and enhanced chemiluminescence.

ecules are poorly translated. Studies in *Xenopus* oocytes have previously shown that nuclear events such as transcription (14, 15) or splicing (11, 37) can affect the translational behavior of specific mRNA molecules. Regulation of translation is most often seen at the level of initiation (38–40). If this were the case then we would not expect to see the mRNA derived from the intronless transcripts associated with polysomes. However, comparable amounts of DHFR mRNA molecules were present in transfectants from both pDCH1P11 and pDCH1P10 and their polysomal distributions were virtually identical (data not shown), suggesting mRNA derived from the intronless transcripts was efficiently recruited into polysomes. We then determined the translational rates for the DHFR protein in transfectants from pDCH1P11 and pDCH1P10 by metabolic labeling assays. Cells were labeled with 150 μCi/ml [^{35}S]methionine and cysteine in methionine- and cysteine-free medium for different periods of time, and radiolabeled DHFR was immunoprecipitated from cytoplasmic extracts. As shown in Fig. 6*A*, the rate of DHFR protein synthesis in pDCH1P10 transfectants was decreased by 2-fold compared with the rate of DHFR in pDCH1P11 transfectants.

DHFR Protein Is Unstable in Transfectants Carrying the Intronless Minigene—In addition to the 2-fold difference in the translational rate of DHFR, the low steady state level of the protein in pDCH1P10 transfectants could be also because of a rapid degradation of the protein that is synthesized from mRNA derived from intronless transcripts.

To characterize the time course of DHFR degradation, we used cycloheximide to stop new protein synthesis and examine the decay of the remaining DHFR protein. Transfectant cells from pDCH1p11 and pDCH1p10 were harvested at 4, 8, 16, and 24-h intervals after the addition of 50 μg/ml cycloheximide and cytoplasmic extracts were prepared. The levels of DHFR were determined by Western blot, as described under "Materials and Methods." The half-life of the DHFR protein in permanent transfectants from the intron-containing *dhfr* minigene was about 25 h, whereas in transfectants from the intronless minigene, DHFR half-life was reduced to about 9 h (Fig. 6*B*), which corresponded to a 64% decrease in the stability of the protein.

Because cycloheximide treatment may have effects on numerous proteins, including synthesis of proteases involved in DHFR degradation, pulse-chase experiments with [^{35}S]methionine and cysteine and immunoprecipitation with anti-hamster DHFR antibody were carried out to confirm the above results. The cells were incubated with 150 μCi/ml [^{35}S]methionine and cysteine for 90 min and chased with 2 mM methionine and 2 mM cysteine for different periods of time. As shown in Fig. 6*C*, the half-life of the DHFR protein in permanent

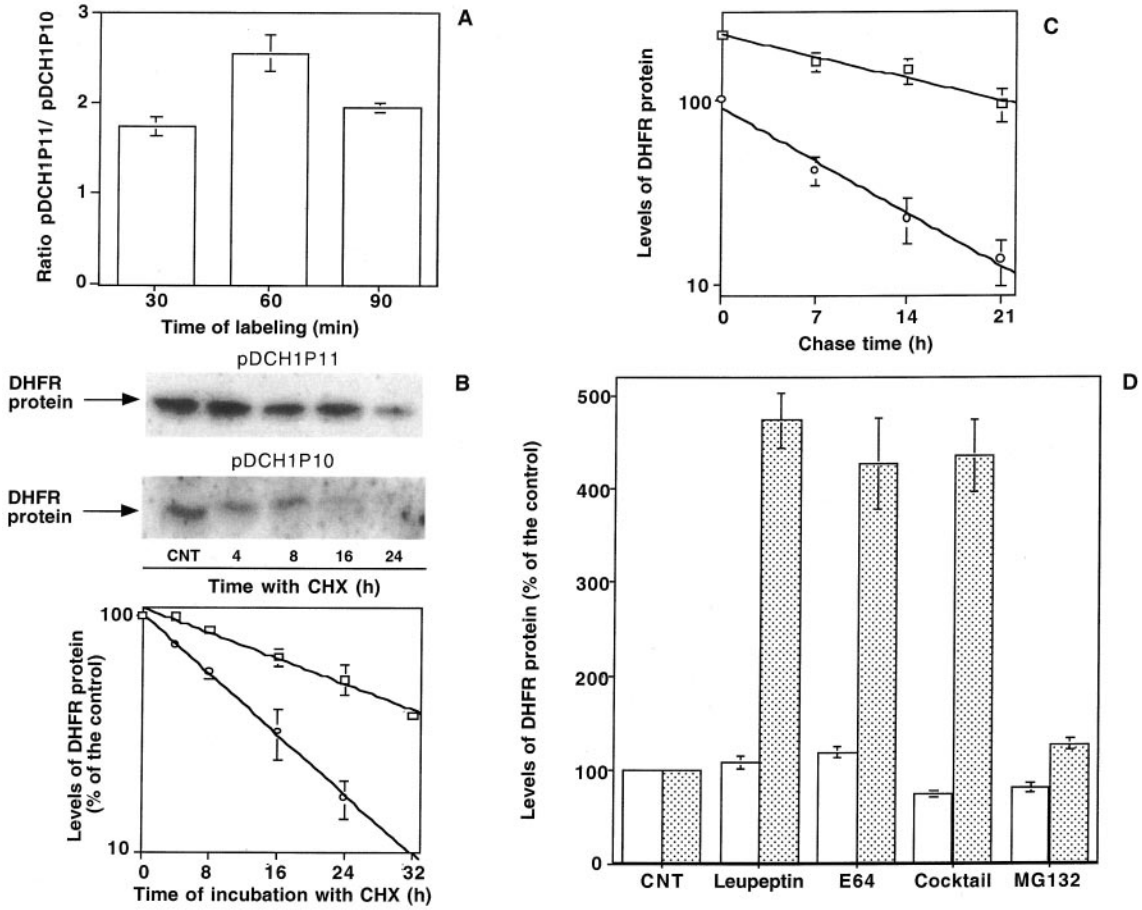

FIG. 6. **Translation rate and stability of DHFR protein in pDCH1P11 and pDCH1P10 transfectants.** *A*, transfectants from pDCH1P11 and pDCH1P10 were pulse-labeled with [^{35}S]Met + Cys for the indicated periods of time. Cells were harvested by trypsinization and cytoplasmic extracts were prepared. DHFR protein was immunoprecipitated with an antibody raised against hamster DHFR. The immunoprecipitated proteins were separated by SDS-PAGE and analyzed by phosphorimaging. Results are expressed as the ratio of DHFR translational rates between pDCH1P11 and pDCH1P10 transfectants. Results correspond to the mean ± S.E. of two independent experiments. *B*, transfectants from pDCH1P11 and pDCH1P10 were incubated with 50 μg/ml cycloheximide for the indicated times, and cytoplasmic extracts were prepared. The levels of DHFR protein were determined by Western blot as described under "Materials and Methods." The *top panel* corresponds to a representative autoradiography of the protein bands, and the quantitation performed by image analysis is shown in the *bottom panel*. Results are the mean ± S.E. of three independent experiments. *C*, transfectants from pDCH1P11 and pDCH1P10 were pulse-labeled for 90 min with [^{35}S]Met + Cys and then chased for different periods of time. After the chase, cells were harvested by trypsinization and cytoplasmic extracts were prepared. DHFR protein was immunoprecipitated with an antibody raised against hamster DHFR. The immunoprecipitated proteins were separated by SDS-PAGE and analyzed by phosphorimaging. Results are expressed as the percentage of DHFR protein levels to those in pDCH1P10 transfectants. Results correspond to the mean ± S.E. of two independent experiments. *D*, transfectants from pDCH1P11 (*open bars*) and pDCH1P10 (*filled bars*) were treated with 50 μM leupeptin, 50 μM E64, a 1:400 dilution of the protease inhibitor mixture for 24 h, or 40 μM MG132 for 6 h. Then, cells were harvested by trypsinization, and cytoplasmic extracts were prepared as described under "Materials and Methods." The levels of DHFR protein were determined by Western blot using an antibody against hamster DHFR. The quantitation was performed by image analysis. Results are the mean ± S.E. of two independent experiments.

transfectants from pDCH1P11 was about 17.5 h, whereas in transfectants from pDCH1P10, DHFR half-life was reduced to about 6.5 h, which corresponded to a 63% decrease in the stability of the protein.

Intracellular proteins can be degraded by three general types of proteolytic reactions, namely lysosomal proteinases, the ubiquitin-proteasome pathway, and the calcium-activated neutral protease (calpain) system (41). To evaluate which proteases could contribute toward the faster degradation of DHFR in pDCH1P10 transfectants, the effect of different protease inhibitors on DHFR protein levels was determined. Cells were incubated with leupeptin, which inhibits lysosomal serine/cysteine proteases (42); E64, a lysosomal cysteine protease inhibitor (43); a protease inhibitor mixture that inhibits serine, cysteine, aspartic, and aminopeptidases; and MG132, an inhibitor of the chymotrypsin-like and peptidyl glutamate sites of the 20 S proteasome (44). After 24 h of treatment either with leupeptin, E64, or the inhibitor mixture or after 6 h of treatment with MG132, cells were harvested by trypsinization and cytoplasmic extracts were prepared and analyzed by Western blot. As shown in Fig. 6*D*, treatment of pDCH1P10 transfectants with leupeptin, E64, or the inhibitor mixture led to more than a 4-fold increase in the levels of DHFR protein, whereas the treatment with the proteasome inhibitor MG132 did not affect the levels of DHFR protein in these cells. The levels of DHFR protein in pDCH1P11 transfectants were not significantly modified by the incubation with the different protease inhibitors.

DISCUSSION

Here we analyzed the role of introns in the production of DHFR protein in transfected CHO cells. We used a set of *dhfr* minigenes containing either *dhfr* intron 1, *aprt* intron 3, *β-globin* intron 1, or no intronic sequence, and we analyzed the three steps of RNA processing in stable transfectants from these constructs. We show that (i) DHFR mRNA was expressed, correctly polyadenylated, and efficiently accumulated in the cytoplasm despite the absence of an intron in the corresponding

minigene, (ii) the presence of an intron in the minigene was a requirement for the accumulation of high levels of DHFR protein, (iii) the effect of an intron on DHFR protein expression was sequence- and position-independent, and (iv) DHFR protein encoded by the intronless minigene was less stable than its counterpart from the intron-containing minigene.

The abundance of DHFR mRNA transcribed for an intronless minigene was analogous to the levels obtained from the corresponding intron-containing minigene (Fig. 3). Several authors have used the *dhfr* gene as a model to establish the effect of introns in RNA processing. The efficiency of an intronless hamster *dhfr* minigene was only 5–10% that of its intron-containing counterpart upon transfection of DHFR-deficient CHO mutant cells (19). Transfections with mouse *dhfr* minigenes containing introns produced at least 10-fold more colonies than did similar transfections with minigenes lacking introns (18). This low transfection efficiency is in agreement with our observations regarding DHFR activity and protein levels in transfectants from a *dhfr* intronless minigene (Fig. 2). However, transfectants produced by a *dhfr* cDNA clone contained very little DHFR mRNA (19), and a mouse *dhfr* intron-containing construct produced 10- to 20-fold more RNA than the corresponding construct without the intronic sequence upon transfection in COS cells (2). The discrepancy observed in the resulting DHFR mRNA levels could be because of the differences in the constructs used throughout these studies. In our case the intronless *dhfr* construct carries 400 bp of the genomic 5′-flank and the inclusion of the *dhfr* promoter increases the efficiency of transfection of a *dhfr* cDNA clone (19). In addition, in our minigenes the intronic sequence was included at the original position of *dhfr* intron 1 or in the 5′-flank. Other authors have demonstrated that the presence of an intron at the 5′-end of the transcript can activate translation (37, 45, 46), which agrees with our results regarding DHFR mRNA and protein levels in transfectants from the 5′-UTR-I1-pDCH1P10 minigene. According to Hawkins (47), introns located 3′ of termination codons are very rare, whereas 111 5′-non-coding exons were found in 328 vertebrate genes. The 3′-end of our constructs included either the endogenous *dhfr* pA1 or an SV40 pA, and DHFR transcripts were correctly polyadenylated at both sites (Fig. 4).

We also show that DHFR mRNA transcribed from an intronless minigene is correctly polyadenylated at the polyadenylation site present in the construct, either the endogenous *dhfr* p(A)1 or an SV40 p(A) site (Fig. 4). These results suggest that in our system polyadenylation occurs in the absence of splicing, in contrast to studies demonstrating that the presence of an intron within a RNA targets that RNA toward the polyadenylation pathway in transient transfections (4, 5). The requirement of a functional 3′-terminal intron for efficient 3′-end formation is supported by studies using cultured cells (6, 7) or cell-free assays (48, 49). In addition, cleavage and polyadenylation appear to be a prerequisite for RNA export to the cytoplasm (50). A poly(A) stretch alone is not sufficient for mRNA export, suggesting that polyadenylation is essential for mRNA export (51). However, DHFR transcripts derived from intronless minigenes are efficiently transported to the cytoplasm *in vitro* after their injection into the nuclei of *Xenopus* oocytes (52–54). In agreement with other reports (45, 46), our results regarding the cellular distribution of DHFR mRNA derived from either an intron-containing or an intronless minigene indicate that RNA export is not affected by splicing.

The abundance of DHFR protein does not correlate with the mRNA levels derived from the intronless minigene. When *dhfr* intron 1 was replaced by heterologous introns, the resulting levels of mRNA and protein suggest that splicing is essential for the translation of the transcript (Fig. 5). Bouvet and Wolffe (14) reported that the presence of an intron had no influence on mRNA synthesis or overall translational efficiency in *Xenopus* oocytes. In contrast, Braddock *et al.* (15) showed that the presence of a functional intron allowed the translation of an *in vitro* transcribed RNA after its injection into the nucleus of *Xenopus* oocytes. In a later report, Matsumoto *et al.* (37) described that intronless mRNA is exported from the nucleus and is inefficiently translated, whereas if the same mRNA enters the splicing pathway, translational efficiency is increased. However, the effect of splicing on the translation of the resulting mRNA is probably limited to a subset of specific genes. In this direction, Lu and Cullen (46) tested the enhancing effects of splicing on the expression of 10 human proteins of different sizes and functions. All 10 genes tested were expressed at higher levels when they encoded an intron in their 5′-UTR, but the degree of intron dependence varied between 35-fold for the β-globin gene and 2-fold in the case of hnRNPK. These authors concluded that the degree of intron dependence is encoded within the cDNA sequence of the gene.

Our results in the pulse experiments indicate that the translational rate of DHFR protein is increased in transfectants from the intron-containing minigene. Nott *et al.* (45) also reported a 2.4-fold increase in translational yield for TP1/Renilla and TCR-β constructs in HeLa cells that could either reflect an increased translatability of the spliced messages or a differential stability of the encoded polypeptide.

The inefficient translation of the intronless transcripts is reminiscent of the mechanism of nonsense-mediated decay (NMD). A post-termination surveillance model has been proposed in which splicing positions a factor(s) at the exon-exon junction of the mRNA that would be encountered by the elongating ribosome, which results in a stable mRNA. In mRNAs with a premature translation termination codon at a position upstream of a critical boundary in the penultimate exon, the factor(s) at the downstream exon-exon junction would be recognized by the hypothetical surveillance complex that scans the mRNA after termination has occurred. As a result of this interaction, the mRNA will be degraded (16). This model explains the necessity of introns and the requirement of translation for cytoplasmic NMD (16, 17). Accordingly, naturally intronless genes (55, 56) or human genes with deleted introns (53) have been shown to be NMD-resistant. Similarly, for an intronless transcript the absence of a proper exon-exon junction complex would result in poor translation. Pre-mRNA splicing generates an mRNP complex distinct from that assembled on the identical mRNA lacking introns (12, 13). We could then envisage a model for translational control, by which mRNAs encoded by intronless minigenes fail to present the proper marks at the exon-exon junctions and the absence of these marks would lead the newly synthesized peptides to degradation. Alternatively, the absence of exon-exon junction marks would determine a secondary structure in the mRNA that, although it allowed association with polysomes, would prevent its translation. The translational control of maternal mRNA during early *Xenopus* development is based on the regulated assembly and disassembly of RNA-binding proteins to mRNA transcripts. The assembly of mRNPs during oogenesis sequesters maternal mRNA in an inert state, such that it is masked from the translational apparatus (57). The translational activation of these masked mRNAs occurs during meiotic maturation and after fertilization. Masked mRNAs are not translated *in vivo* but can be efficiently translated *in vitro*, provided that they have previously been subjected to deproteinization (14). The translational rate of DHFR protein in transfectants from the intron-containing minigene indicates that spliced mRNAs

exhibit higher translational rates than do intronless transcripts and agrees with the influence of a proper exon junction complex in the translation of a given mRNA molecule. The enhancement of translation as a consequence of the deposition of an EJC or other alteration in mRNP structure during splicing has also been suggested by other authors (45, 46).

The regulation of translation has been widely studied at the level of the mRNA substrate, and the influence of the different steps in RNA processing such as transcription, polyadenylation, splicing, and export in translation efficiency has been established using several models. However, cells possess other levels of quality control, such as the system of chaperones and proteases to repair or remove most forms of damaged proteins. About 20% of newly synthesized polypeptides are degraded; this highly unstable fraction may comprise incomplete proteins resulting from errors in transcription or translation (58). Our results on DHFR protein half-life, either from the pulse-chase experiments or using cycloheximide, and on the effects of different protease inhibitors (Fig. 6) suggest that the DHFR protein encoded by the intronless minigene may fold in an unstable conformation that would eventually lead to degradation by the lysosomes. In fact, it has been shown *in vitro* that DHFR is taken up into lysosomes where it is degraded by lysosomal cathepsins (59) and that the efficient transport of the protein from the cytosol to the lysosomes depends on an unfolded conformation (60). *In vivo*, the chaperone-mediated autophagic pathway, one of the mechanisms of lysosomal protein degradation, is activated at least in part to transport some DHFR molecules from the cytosol into lysosomes (60).

In summary, the absence of splicing does not affect the levels of correctly polyadenylated cytoplasmic DHFR mRNA. The mRNA molecules derived from the intronless construct undergo translation, although at a lower rate than mRNA transcripts that have been subjected to splicing. In addition, *dhfr* pre-mRNA splicing influences the stability of the resulting DHFR protein and thus mediates its post-translational control through a mechanism of degradation that involves lysosomes.

Acknowledgments—We thank Dr. L. Chasin for providing the hamster *dhfr* minigenes and the antibody against hamster DHFR protein and for critical suggestions, Dr. J. Manley for suggesting the U6 RNA control, and R. Rycroft from the Language Advisory Service (S.A.L.) for correcting the English manuscript.

REFERENCES

1. Brinster, R. L., Allen, J. M., Behringer, R. R., Gelinas, R. E. & Palmiter, R. D. (1988) *Proc. Natl. Acad. Sci. U. S. A.* **85,** 836–840
2. Buchman, A. R. & Berg, P. (1988) *Mol. Cell. Biol.* **8,** 4395–4405
3. Collis, P., Antoniou, M. & Grosveld, F. (1990) *EMBO J.* **9,** 233–240
4. Huang, M. T.-F. & Gorman, C. M. (1990) *Nucleic Acids Res.* **18,** 937–947
5. Pandey, N. B., Chodchoy, N., Liu, T. J. & Marzluff, W. F. (1990) *Nucleic Acids Res.* **18,** 3161–3170
6. Nesic, D., Chang, J. & Maquat, L. E. (1993) *Mol. Cell. Biol.* **13,** 3359–3369
7. Nesic, D. & Maquat, L. E. (1993) *Genes Dev.* **8,** 363–375
8. Lou, H., Gagel, R. F. & Berget, S. M. (1996) *Genes Dev.* **10,** 208–219
9. Cooke, C., Hans, H. & Alwine, J. C. (1999) *Mol. Cell. Biol.* **19,** 4971–4979
10. Ryu, W.-S. & Mertz, J. E. (1989) *J. Virol.* **63,** 4386–4394
11. Meric, F., Searfoss, A. M., Wormington, M. & Wolffe, A. P. (1996) *J. Biol. Chem.* **271,** 30804–30810
12. Luo, M. J. & Reed, R. (1999) *Proc. Natl. Acad. Sci. U. S. A.* **96,** 14937–14942
13. Le Hir, H., Izaurralde, E., Maquat, L. E. & Moore, M. J. (2000) *EMBO J.* **19,** 6860–6869
14. Bouvet, P. & Wolffe, A. P. (1994) *Cell* **77,** 931–941
15. Braddock, M., Muckenthaler, M., White, M. R. H., Thorburn, A. M., Sommerville, J., Kingsman, A. J. & Kingsman, S. M. (1994) *Nucleic Acids Res.* **22,** 5255–5264
16. Zhang, J., Sun, X., Qian, Y. & Maquat, L. E. (1998) *RNA* **4,** 801–815
17. Sun, X., Moriarty, P. M. & Maquat, L. E. (2000) *EMBO J.* **19,** 4734–4744
18. Gasser, C. S., Simonsen, C. C., Schilling, J. W. & Schimke, R. T. (1982) *Proc. Natl. Acad. Sci. U. S. A.* **79,** 6522–6526
19. Venolia, L., Urlaub, G. & Chasin, L. A. (1987) *Somat. Cell. Genet.* **13,** 491–504
20. Crouse, G. F., Stivaletta, L. A. & Smith, M. L. (1988) *Nucleic Acids Res.* **16,** 7025–7042
21. Kessler, O., Jiang, Y. & Chasin, L. A. (1993) *Mol. Cell. Biol.* **13,** 6211–6222
22. Gossen, M. & Bujard, H. (1992) *Proc. Natl. Acad. Sci. U. S. A.* **89,** 5547–5551
23. Kessler, O. & Chasin, L. A. (1996) *Mol. Cell. Biol.* **16,** 4426–4435
24. Urlaub, G., Mitchell, P. J., Kas, E., Funanage, V. L., Myoda, T. T & Hamlin, J. L. (1986) *Somat. Cell Mol. Genet.* **12,** 555–566
25. Wigler, M., Pellicer, A., Silverstein, S., Axel, A., Urlaub, G. & Chasin, L. A. (1979) *Proc. Natl. Acad. Sci. U. S. A.* **76,** 1373–1376
26. Luskey, M. & Botchan, M. R. (1984) *Cell* **36,** 391–401
27. Noé, V., Alemany, C., Chasin, L. A. & Ciudad, C. J. (1998) *Oncogene* **16,** 1931–1938
28. Laemmli, U. K. (1970) *Nature* **227,** 680–685
29. Sallés, F. J., Richards, W. G. & Strickland, S. (1999) *Methods* **17,** 38–45
30. Noé, V., Ciudad, C. J. & Chasin, L. A. (1999) *J. Biol. Chem.* **274,** 27807–27814
31. Lee, F., Mulligan, R., Berg, P. & Ringold, G. (1981) *Nature* **294,** 228–232
32. Rousseau, D., Kaspar, R., Rosenwald, I. Gehrke, L., & Sonenberg, N. (1996) *Proc. Natl. Acad. Sci. U. S. A.* **93,** 1065–1070
33. Hamm, J. & Mattaj, I. W. (1989) *EMBO J.* **8,** 4153–4158
34. Muckenthaler, M., Gunkel, N., Stripecke, R. & Hentze, M. W. (1997). *RNA* **3,** 983–995
35. Preiss, T., Muckenthaler, M. & Hentze, M. W. (1998) *RNA* **4,** 1321–1331
36. de Moor, C. H. & Richter, J. D. (2001) *Int. Rev. Cytol.* **203,** 567–608
37. Matsumoto, K., Wassarman, K. M. & Wolffe, A. P. (1998) *EMBO J.* **17,** 2107–2121
38. Gray, N. K. & Wickens. M. (1998) *Annu. Rev. Cell Dev. Biol.* **14,** 399–458
39. Preiss, T. & Hentze, M. W. (1999) *Curr. Opin. Genet. Dev.* **9,** 515–521
40. Gingras, A. C., Raught, B. & Sonenberg, N. (2001) *Genes Dev.* **15,** 807–826
41. Dice, J. F. (1987) *FASEB J.* **1,** 349–357
42. Seglen, P. O., Grinde, B. & Solheim, A. E (1979). *Eur. J. Biochem.* **95,** 215–335
43. Moriyama, T., Sather, S. K., Mcgee, T. P. & Simoni, R. D. (1998) *J. Biol. Chem.* **273,** 22037–22043
44. Lee, D. H. & Goldberg, A. L. (1996) *J. Biol. Chem.* **271,** 27280–27284
45. Nott, A., Meislin, S. H. & Moore, M. J. (2003) *RNA* **9,** 607–617
46. Lu, S. & Cullen, B. R. (2003) *RNA* **9,** 618–630
47. Hawkins, J. D. (1988) *Nucleic Acids Res.* **16,** 9893–9908
48. Niwa, M., Rose, S. D. & Berget, S. M. *Genes Dev.* (1990) **4,** 1552–1559
49. Niwa, M. & Berget, S. M. *Gene Expr.* (1991) **1,** 5–14
50. Eckner, R., Ellmeier, W. & Birnstiel, M. L. (1991) *EMBO J.* **10,** 3513–3522
51. Huang, Y. & Carmichael, G. G. (1996) *Mol. Cell. Biol.* **16,** 1534–1542
52. Pasquinelli, A. E., Ernst, R. K., Lund, E., Grimm, C., Zapp, M. L., Rekosh, D., Hammarskjold, M. L. & Dahlberg, J. E. (1997) *EMBO J.* **16,** 7500–7510
53. Ullman, K. S., Shah, S., Powers, M. A. & Forbes, D. J. (1999) *Mol. Biol. Cell* **10,** 649–664
54. Rodrigues, J. P., Rode, M., Gatfield, D., Blencowe, B. J., Carmo-Fonseca, M. & Izaurralde, E. (2001). *Proc. Natl. Acad. Sci. U. S. A.;* **98,** 1030–1035
55. Maquat, L. E. & Li, X. (2001) *RNA* **7,** 445–456
56. Brocke, K. S., Neu-Yilik, G., Gehring, N. H., Hentze, M. W. & Kulozik, A. E. (2002) *Hum. Mol. Genet.* **11,** 331–335
57. Standart, N. & Jackson, R. (1994) *Curr. Biol.* **4,** 939–941
58. Wickner, S., Maurizi, M. R. & Gottesman, S. (1999) *Science* **286,** 1888–1893
59. Terlecky, S. R. & Dice, J. F. (1993) *J. Biol. Chem.* **268,** 23490–23495
60. Salvador, N., Aguado, C., Horst, M. & Knecht, E. (2000) *J. Biol. Chem.* **275,** 27447–27456